 Human Molecular Genetics, 2002, Vol. 11, No. 21 2615–2624

The disintegrin/metalloprotease ADAM 10 is essential for Notch signalling but not for α-secretase activity in fibroblasts

Dieter Hartmann[1,†], Bart de Strooper[1,†], Lutgarde Serneels[1], Katleen Craessaerts[1], An Herreman[1], Wim Annaert[1], Lieve Umans[2], Torben Lübke[3], Anna Lena Illert[3], Kurt von Figura[3] and Paul Saftig[4,*]

[1]Center for Human Genetics KU Leuven and Flanders Interuniversity Institute for Biotechnology, VIB 4 and [2]Department of Developmental Biology KU Leuven, VIB 7 (Celgen), Herestraat 49, 3000 Leuven, Belgium, [3]Zentrum Biochemie und Molekulare Zellbiologie, Abteilung Biochemie II, Universität Göttingen, 37073 Göttingen, Germany and [4]Biochemisches Institut der Christian-Albrecht-Universität Kiel, Olshausenstrasse 40, D-24118 Kiel, Germany

Received June 6, 2002; Revised and Accepted August 1, 2002

The metalloprotease ADAM 10 is an important APP α-secretase candidate, but *in vivo* proof of this is lacking. Furthermore, invertebrate models point towards a key role of the ADAM 10 orthologues Kuzbanian and sup-17 in Notch signalling. In the mouse, this function is, however, currently attributed to ADAM 17/TACE, while the role of ADAM 10 remains unknown. We have created ADAM 10-deficient mice. They die at day 9.5 of embryogenesis with multiple defects of the developing central nervous system, somites, and cardiovascular system. *In situ* hybridization revealed a reduced expression of the Notch target gene *hes-5* in the neural tube and an increased expression of the Notch ligand *dll-1*, supporting an important role for ADAM 10 in Notch signalling in the vertebrates as well. Since the early lethality precluded the establishment of primary neuronal cultures, APPsα generation was analyzed in embryonic fibroblasts and found to be preserved in 15 out of 17 independently generated ADAM 10-deficient fibroblast cell lines, albeit at a quantitatively more variable level than in controls, whereas a severe reduction was found in only two cases. The variability was not due to differences in genetic background or to variable expression of the alternative α-secretase candidates ADAM 9 and ADAM 17. These results indicate, therefore, either a regulation between ADAMs on the post-translational level or that other, not yet known, proteases are able to compensate for ADAM 10 deficiency. Thus, the observed variability, together with recent reports on tissue-specific expression patterns of ADAMs 9, 10 and 17, points to the existence of tissue-specific 'teams' of different proteases exerting α-secretase activity.

INTRODUCTION

The abnormal proteolytic processing of amyloid precursor protein (APP) leading to an increased Aβ42/Aβ40 ratio is a central step in the pathogenesis of Alzheimer's disease (AD) (1–3). APP proteolysis has recently been recognized as a special case of regulated intramembrane proteolysis (RIP), a process that generates intra- and/or extracellular fragments from transmembrane proteins involved in signal transduction (4,5). The main feature of protein 'RIPping' is the sequence of an initial regulated ectodomain shedding (initiated, for instance, by ligand binding) that triggers an 'unregulated' cleavage of the remaining C-terminal stubs within their transmembrane region to liberate the intracellular domain of the protein. This fragment can then be targeted to the nucleus to regulate gene transcription (6,7).

As a peculiarity of APP, ectodomain shedding can be performed by two different enzymatic activities termed α- and β-secretase, initiating either the amyloidogenic (β-secretase) or the quantitatively dominating non-amyloidogenic (α-secretase) pathway (8). In either case, APP processing is completed by γ-secretase cleavage (3), generating the APP intracellular domain (AICD) (9). γ-Secretase appears to be a multiprotein complex, the active center of which may be formed by

*To whom correspondence should be addressed. Tel: +49 4318802216; Fax: +49 4318802238; Email: psaftig@biochem.uni-kiel.de
†The authors wish it to be known that, in their opinion, the first two authors should be regarded as joint First Authors.

presenilins (PS) 1 and 2 (10–20). Likewise, β-secretase has recently been identified as a novel, membrane-bound aspartyl protease termed BACE (21).

The definitive identification of α-secretase, in contrast, has remained controversial. This is surprising, since α-secretase was the first proteolytic activity identified to cleave APP (20). The need for a proper identification of α-secretase(s) is likely to expand, since therapeutic approaches such as cholinergic drugs (22) and HMG-CoA reductase inhibitors (see below) appear to act at least partially via stimulation of this activity.

Several enzymes have been proposed to contribute to α-secretase activity, including the proteasome (23), cathepsin B (24), the prohormone convertase PC 7 (25), GPI-linked aspartyl proteases (26) and the β-secretase-related protease BACE 2 (27,28). The most consistent and convincing data implicate metalloproteases of the ADAM family, i.e. ADAM 17/TACE (29), ADAM 10/Kuzbanian (30,31) and ADAM 9/meltrin γ (32). ADAM 17-deficient fibroblasts derived from knockout mice show a normal basal APP secretion, which, however, can no longer be stimulated by PKC (29). This enzyme thus plays a role only in the regulatory component of the α-secretase processing of APP in fibroblasts. However, within the central nervous system (CNS), ADAM 17 is expressed in endothelia and glia (33), but is absent from most neurons, which probably reduces its importance for AD pathogenesis and therapy (34).

ADAM 10 and ADAM 9, on the other hand, increased constitutive and regulated secretion of APPsα in co-transfected cells (30,32). ADAM 10 furthermore cleaves synthetic substrates mimicking the α-secretase site, and a dominant-negative form of ADAM 10 interfered with endogenous α-secretase processing in HEK cells (30). Furthermore, it is well expressed in neurons throughout the CNS (34). The cholesterol sensitivity of α-secretase may be explained by effects on ADAM 10 (35), providing a potentially important link to the currently envisaged use of HMG-CoA reductase inhibitors to treat AD (36).

Both ADAM 17 and ADAM 10 may also fulfil important functions in the Notch signalling pathway by performing the 'site2' cleavage essential for Notch receptor activation upon ligand binding, or by shedding the Notch ligand Delta from the cell surface in *Drosophila* (37–39). Both Kuzbanian (ADAM 10)-deficient flies and sup-17 (ADAM 10) null mutation in *Caenorhabditis elegans* cause phenotypes related to Notch (lin-12) loss of function, further substantiating mainly the role of ADAM 10 orthologues in Notch signalling in invertebrates (38,39).

In the vertebrates, however, the situation is unclear. While expression of a dominant-negative *Drosophila kuzbanian* variant in *Xenopus* results in phenotypic alterations suggestive of impaired (X)Notch function, two groups recently failed to demonstrate a role for ADAM 10 in Notch site2 cleavage in murine cells (40,41). Particularly confusing in this regard is that they found, in contrast, that ADAM 17 is the protease responsible for Notch site2 cleavage, while the phenotype of ADAM 17-deficient mice is not related to any Notch or Notch ligand loss of function (42,43). Thus, we are confronted here with apparent discrepancies between the available *in vitro* and *in vivo* observations. To analyze in further detail the potential contribution of ADAM 10 in α-secretase processing of APP and its possible physiological role in the Notch signalling pathway in vertebrates, we have generated ADAM 10-deficient mice.

RESULTS

Targeted disruption of the *ADAM 10* gene in mice

The open reading frame (ORF) of the *ADAM 10* gene region was disrupted by insertion of a *neo* cassette at nucleotide position 187, corresponding to amino acid residue 62 of ADAM 10. Using the 5′ external probe A (Fig. 1A) one of 96 embryonic stem (ES) cell clones displayed an additional *Sac*I DNA restriction fragment demonstrating homologous recombination in one of the *ADAM 10* alleles (Fig. 1B). All of the nine chimeric males that were generated transmitted the mutated allele through the germline. Heterozygous mice exhibited a normal phenotype and normal fertility (data not shown). Since no living *ADAM* $10^{-/-}$ mice were obtained, *ADAM* $10^{-/-}$ embryos were evaluated at different stages of development. At day 9.5 of embryogenesis (E 9.5), *ADAM* $10^{-/-}$ embryos were present in a Mendelian frequency (not shown), as evaluated by an exon-specific PCR (Fig. 1C). The absence of transcription (Fig. 2A and B) and translation (Fig. 2C) of the *ADAM 10* gene in ADAM $10^{-/-}$ fibroblasts was further confirmed using RT–PCR and northern and western blotting experiments (Fig. 1). No viable *ADAM* $10^{-/-}$ embryos were obtained beyond E 9.5.

ADAM 10-deficient embryos exhibit multiple defects related to Notch signalling

ADAM 10-deficient embryos at E 9.5 reached about two-thirds of the normal size, whereby the body region distal to the forelimb buds was most severely affected by the growth retardation. The most salient features were foreshortened forebrain anlage, abnormal hindbrain flexure, enlarged pericardial sacs that occasionally expanded to extreme sizes, reduced first branchial arch and conspicuous extracorporal mesenchymal swellings at the insertion of the umbilical cord (Fig. 2A and B). Development of the heart was severely retarded, its morphology corresponding at E 9.5 to an E 7.5–E 8.0 stage just after tube fusion (Fig. 2C and D). Nevertheless, heartbeat was observed in most of the embryos, and only by this criterion living embryos were analyzed further.

The fusing neural tubes were characterized by highly irregularly shaped lateral walls, which (similar to the enlarged pericardial sac) were also described in other mouse models with impaired Notch signalling (Fig. 2E and F) (44).

Somitogenesis, another characteristic target of Notch signalling defects, was severely disturbed (Fig. 2G–J). Only the rostral four or five pairs of somites appeared relatively normal, albeit irregular in size and less well delineated. The caudalmost 'normal' somite was regularly followed by a protruding bulge of paraxial mesoderm, corresponding to fused somite anlagen containing material of several segments (Fig. 2) grouped around two or three fused blastocoel cavities. Further caudal to this fused region, a few small but normally spaced somites were again observed. The internal architecture of the somites

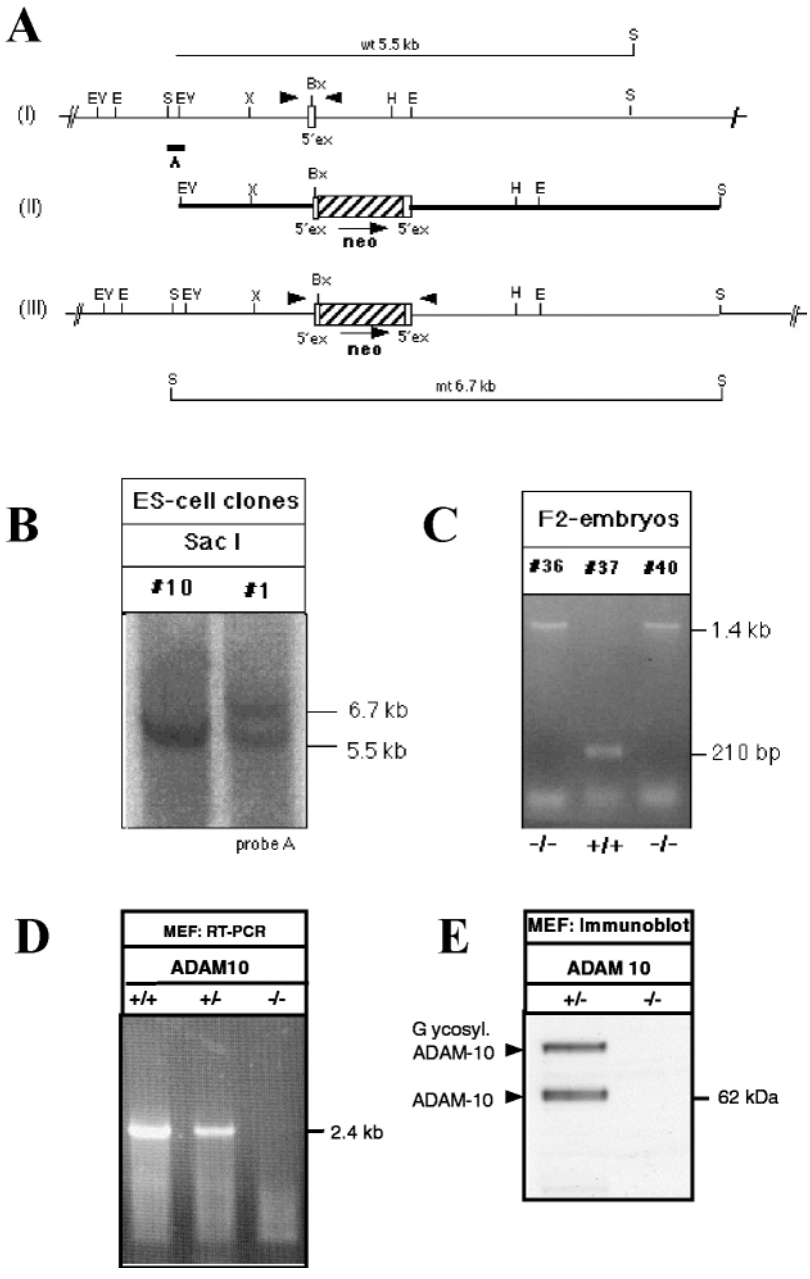

Figure 1. Generation of ADAM 10-deficient mice. (**A**) Strategy for inactivation of the *ADAM 10* gene by homologous recombination in ES cells. (I) Partial structure of the genomic locus representing about 8 kb of the *ADAM 10* gene region. A 5′ exon is indicated by an open box; flanking introns are indicated by solid lines. The bar designated A denotes the DNA probe used for Southern blot analysis. (II) Targeting vector pBS–ADAM 10(neo) with 5.3 kb homology to the *ADAM 10* gene locus. The *neo* cassette was inserted into a *Bgl*II restriction site in the 5′ exon. The arrow marks the direction of transcription of the *neo* gene. (III) Predicted *ADAM 10* gene locus after homologous recombination. (**B**) Southern blot analysis of ES cell clones. The 5′ probe *A* was hybridized to *Sac*I-digested genomic DNA. The additional 6.7 kb DNA fragment indicates a targeted allele. (**C**) PCR analysis of mouse embryonic DNA with an exon-specific PCR amplifying a 0.2 kb fragment in +/+ and a 1.8 kb fragment in −/− mice, respectively. (**D**) Reverse-transcriptase analysis of *ADAM 10* expression. In RNA from +/+ and +/− embryonic fibroblasts, a 2.4 kb *ADAM 10*-specific cDNA was amplified, indicating *ADAM 10* transcription. (**E**) Western blot analysis of ADAM 10 expression using a polyclonal antiserum against the C-terminal part of mouse ADAM 10.

developed at least to the initial stage of separation of the sclerotome from the dermatomyotome. This is well beyond the Notch-independent somitomeric stage (result not shown). Interestingly, no obvious abnormality was observed in other structures expressing high levels of Notch receptors, such as the otic vesicle.

Analysis of expression of genes related to the Notch pathway was performed by *in situ* hybridization using probes against *dll-1*, which encodes one of the major ligands of Notch receptors, against *notch-1* itself and against *hes-5*, which encodes a basic helix–loop–helix transcription factor that is activated by Notch signaling (Fig. 3). *hes-5* was prominently present in the

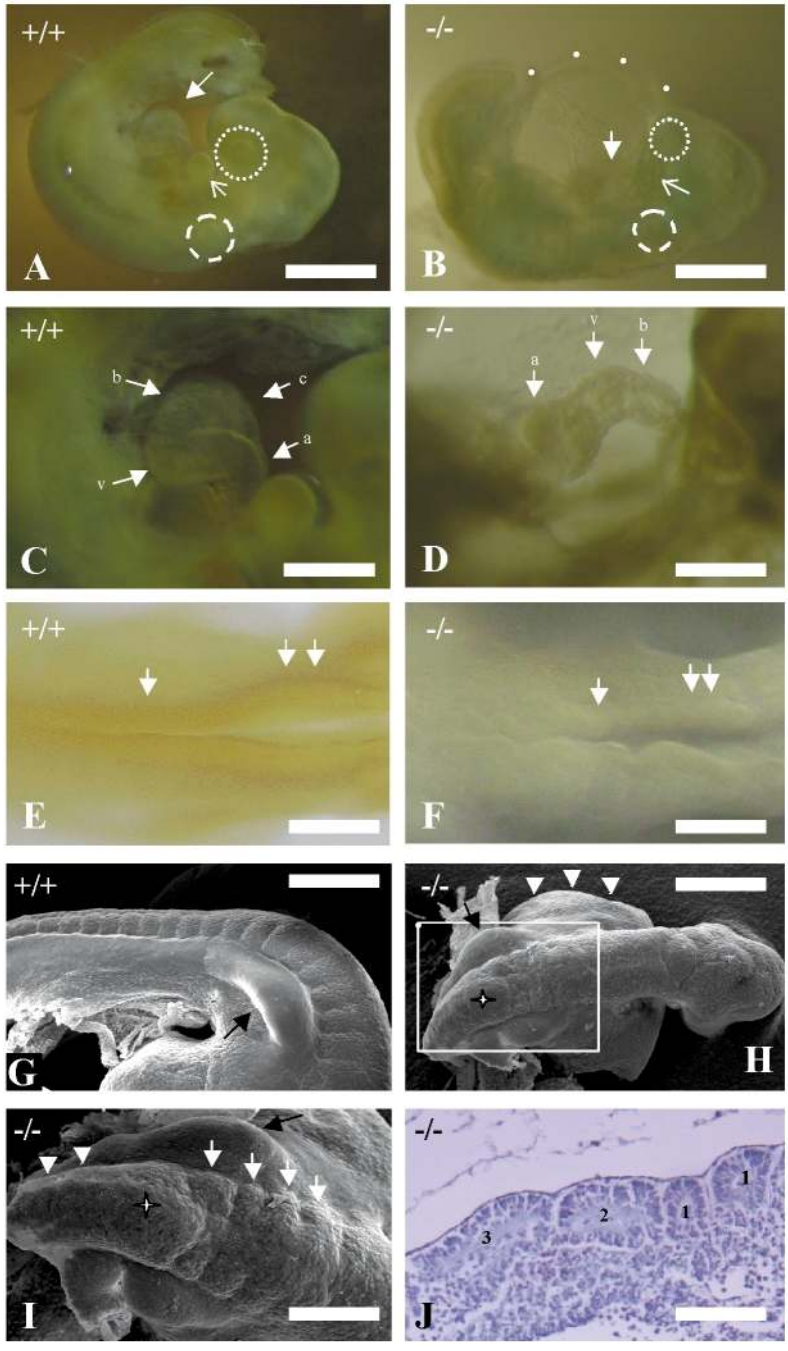

Figure 2 Phenotype of ADAM 10-deficient mice. E 9.5 embryos are displayed, the latest stage at which living (as judged by visible heartbeat) *ADAM 10*$^{-/-}$ embryos could be obtained. (**A** and **B**) Knockout mice (B) reach about two-third of the size of littermate controls (A). The most salient features are the underdevelopment of the caudal body region, a grossly enlarged pericardial sac (dotted line) containing an underdeveloped heart, and a smaller and foreshortened telencephalic anlage (dotted and dashed circles indicate optic cup and otic pit as reference points). The mandibular portion of the first branchial arch (open arrow) is substantially reduced in size. (**C**) and (**D**) Heart development is retarded and comparable to that of an E 7.5–E 8.0 mouse embryo just after fusion of the endocardial tubes. The wild-type littermate shows the characteristic folding of the heart into primordial atrial (a), ventricular (v) and arterial [bulbus (b) and conus (c)] compartments present on E 9.5, which are arranged in a linear fashion in knockouts. Heartbeat was nevertheless regularly recorded. (**E**) and (**F**) The neural tube was characterized by a highly irregular shape of its neuroepithelial wall both in the spinal chord (arrow) and in the lower brain stem (double arrow) region in ADAM 10-deficient mice. (**G**)–(**J**) A peculiar defect was found in the segmentation of the paraxial mesoderm [see (G) and (H) for a survey; the white rectangle in (H) corresponds to the region shown in (I)]. The forelimb bud is indicated by a black arrow in (G), (H) and (I) to provide a point of reference. In (H) and (I), only the first four or five segments are formed as normal, albeit somewhat irregular and too small [indicated by individual arrows in (I)]. This is followed by a bulge of tissue [white star in (H) and (I)] corresponding to fused somites extending over two or three segment lengths. In (J), this region is shown in a paramedian sagittal section through the paraxial mesoderm, covering two rostral somites of normal length (indicated by a '1' in the somitocoel) and following fused somite material surrounding cavities of roughly double ('2') and triple ('3') length. Thereafter segmentation was again (albeit in an irregular diminished pattern) recognizable [white arrowheads in (I)]. Note also the enormous size of the pericardial sac [white arrowheads in (H)].

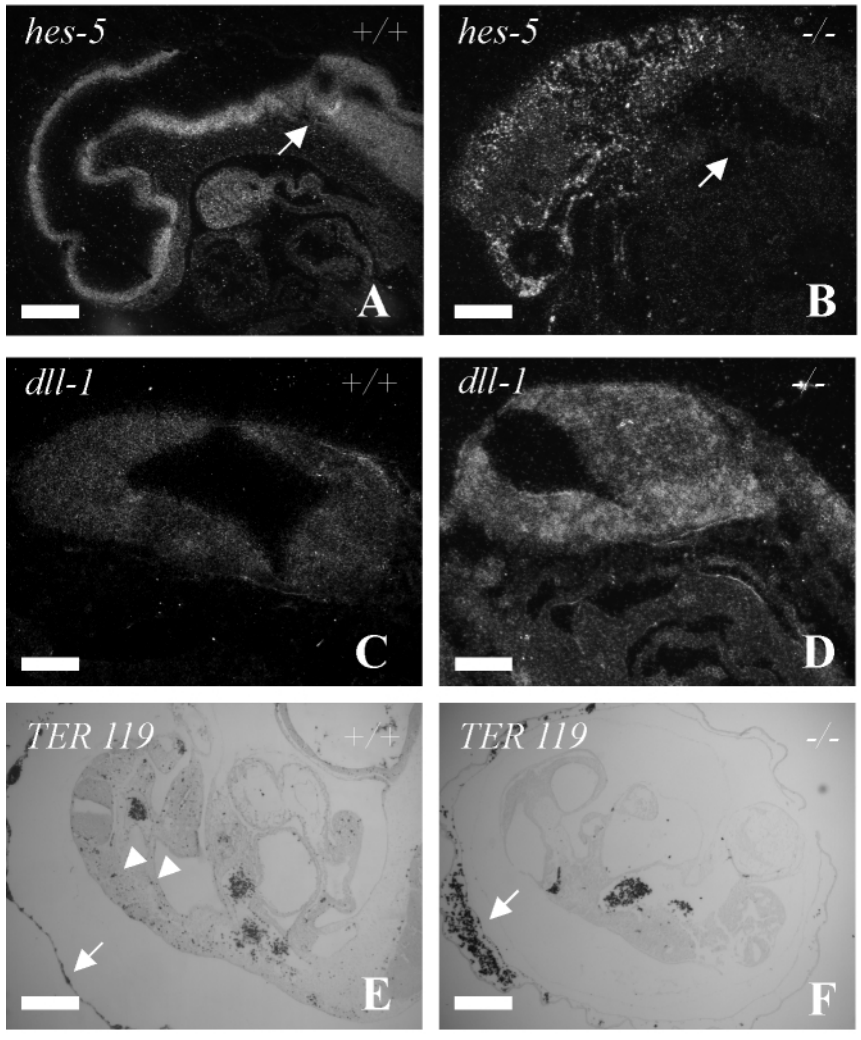

Figure 3. Expression of notch target genes and hematopoiesis in E 9.5 embryos. In wild-type littermates, *hes-5* was expressed at high levels along the entire neuraxis (**A**), whereas a disorganized and reduced pattern of expression was found in knockout mice (**B**). *hes-5* expression was absent in the caudal neural tube/spinal cord anlage. The white arrow indicates the hindbrain–spinal cord junction in both specimens. (**C**) and (**D**) *dll-1* expression is moderately increased in the entire CNS, here shown for the mesencephalic anlage. (**E**) and (**F**) TER 119, an erythroid lineage marker encompassing all stages of red blood cell development, was used to stain the hematopoietic compartment and red blood cells in the yolk sac and within the embryo proper. Blood cells within the control E 9.5 embryo (E) distribute within the main vascular trunks as well as in smaller vessels, for example the segmental branches between somites that are generated at this stage of development (arrowheads). Such vessels are apparently absent in littermate ADAM 10-deficient embryos (F), in which blood cells were confined to main vessels only. In addition, ADAM 10-deficient mice feature drastically enlarged, almost sinusoidal yolk sac vessels crammed with forming blood cells (arrows).

neuroepithelium along the entire neuraxis in wild-type embryos (Fig. 3A and B). In ADAM 10-deficient littermates the expression pattern of *hes-5* in the forebrain and brain stem was severely disorganized, whereas its expression in the spinal cord anlage was reduced below detection level. Notch ligand *dll-1* gene expression, which is normally downregulated by Notch signalling via a negative-feedback mechanism, was upregulated in the CNS anlage (Fig. 3C and D), further indicating disturbed Notch signalling in these mice. The pattern and intensity of *notch-1* expression was unchanged as compared with controls (not shown).

Similar to other knockout models with a more generalized (*notch-1*/*notch-4* double-knockout mice) or putatively total (*PS1/2* double-knockout mice) inactivation of Notch signalling (44,45), yolk sacs of ADAM 10-deficient embryos featured enlarged extraembryonic blood vessels filled with large numbers of embryonic erythrocytes and their progenitors. The most compelling feature of defective intraembryonic vasculogenesis was the virtual absence of smaller aortic branches, for example the intersegmental arteries passing between the somites (Fig. 3E and F).

APPsα secretion is preserved in ADAM 10-deficient murine embryonic fibroblasts

Since the early lethality excluded the establishment of neuronal cultures, we have generated embryonic fibroblast cell lines from wild-type, heterozygous and knockout embryos to analyze APP processing. In order to exclude a potential influence of the genetic background on the biochemical

characteristics of the ADAM 10 deficiency, this was done separately for two different outbred strains (CD1 × 129SV and C57 B6 × 129SV) and for a pure 129SV inbred background. In total, 17 ADAM 10-deficient fibroblast cell lines (7 of the CD1 outbred background, 7 of the C57 outbred background and 3 of the 129SV inbred background) were generated in addition to wild-type and heterozygous controls derived from the respective littermates.

In the vast majority of the ADAM 10-deficient fibroblast cell lines (15 out of 17), the capacity for APP α-secretase cleavage was preserved (Fig. 4). Likewise, ADAM 10-deficient ES cells had a preserved capacity for APP cleavage (not shown). However, in comparison with the fairly uniform amount of APP fragments generated by wild-type cells, α-secretase activity in knockout cell lines was quantitatively more heterogeneous and sometimes even elevated above control level. This was also observed in cell lines derived from a homogenous inbred background (129SV).

An almost-complete loss of α-secretase activity [reduction of C-terminal fragment (CTF) formation below 5% of the control value and a comparable dramatic reduction of APPsα in the supernatant] was only observed in two cell lines (see Fig. 4C and D). When assayed for the effect of the phorbol esters PMA and PDBU on APPsα secretion, it turned out that in the 'secretory' ADAM 10-deficient cell lines, PMA-inducible activity was maintained (Fig. 4B). Conversely, the 'APPs non-secretory' lines had lost both components of α-secretase (Fig. 4D). Notably, the APPsα secretion properties remained stable for a given cell line over an extended time in culture (up to about 30 passages). The absence of β-secretase generated APP CTFs or APPsβ in these experiments was anticipated, since the bulk of APP processing in murine fibroblasts is mediated by α-secretase.

Western blot analysis of the cell lines for the other candidate α-secretases ADAMs 9 and 17 did not reveal any consistent difference between wild-type and 'APPs secretory' and 'APPs non-secretory' *ADAM 10*-knockout cell lines (Fig. 4A′ and C′), i.e. these other candidate α-secretases were present in similar amounts in all wild-type as well as 'secretory' and 'non-secretory' knockout cell lines investigated.

DISCUSSION

We have generated ADAM 10-deficient mice to investigate the contribution of this enzyme to α-secretase activity and Notch signalling. In contrast to previous *in vitro* studies that clearly favored ADAM 10 as a major α-secretase (30,31,35) responsible for both constitutive and regulated α-cleavage, both fractions of α-secretase activity were preserved in the majority of the ADAM 10-deficient cell lines (albeit at a less constant level as compared with controls) and almost lost in only 2 out of 17 lines generated. Whereas these data clearly and unexpectedly show that ADAM 10 (at least in embryonic fibroblasts) is not essential for APP α-cleavage, the observed variability also underscores an essential methodological aspect, i.e. not to rely on only a few or even single cell lines for the reliable biochemical analysis of APPsα secretion in knockout mice.

The most straightforward explanation for the disparate effects of the *ADAM 10* knockout on APPs secretion would be that this protease indeed participates in APP α-cleavage, but that its contribution is either not substantial or can be readily replaced by other α-secretases likewise present in the cells. Thereby, an imprecise regulation of such a compensation could explain the quantitative differences observed between the individual cell lines. In this context, the only two ADAM 10-deficient cell lines exhibiting an almost complete loss of APP secretion could represent the other extreme of an 'undercompensation', thus underscoring at least a potentially critical contribution of ADAM 10 to APPSα secretion.

The expression level of the two other most cited α-secretase candidates, namely ADAMs 9 and 17 (29,32), remained unchanged even in *ADAM 10*-knockout cells that have retained or even increased their capacity for α-secretase cleavage. It remains of course possible that post-translational regulatory mechanisms are involved in the compensation for loss of ADAM 10 function. Such mechanisms—partially mediated by p38 and MAP kinase—regulate the related metalloprotease-mediated shedding of growth factors (46). For APP secretion, similar kinase-mediated pathways can be triggered by Wnt/dishevelled signalling (47). The possibility that variations in the genetic background of the cells cause the variations in compensation is unlikely, since they were also observed in cell lines derived from pure 129SV inbreeds.

Owing to the embryonic lethality of the knockout mice for *ADAM 17* [lethal in late pregnancy (43)] and *ADAM 10* (lethal at E 9.5—this paper), APP processing has been analyzed in fibroblast cell lines instead of primary neuronal cultures. Especially for the *ADAM 10* knockouts described here, this was inevitable, since the embryos died at a stage preceding neuron production. In order to draw conclusions regarding the relative importance of α-secretase candidates for the CNS, one has, however, to take into account the tissue distribution of candidate α-secretases. In the CNS, ADAM 17 is mostly found in endothelia and possibly glia (33), but only in a small number of neurons (34). In contrast, ADAMs 9 and 10 are highly expressed in neurons (34). Thus, data derived from fibroblasts are prone to underestimate the contribution of ADAM 10 to APPα cleavage in the brain. Recently, *ADAM 9*-knockout mice have been generated that display an overall-normal phenotype, in contrast to the *ADAM 10* mice described in the present paper (48). In neuronal cultures derived from these mice, α-secretase activity is preserved, further underscoring the concept that it is probably not a single enzyme but rather a group of enzymes that are responsible for APPsα secretion. It is obvious now that the effect of combined deficiencies should be investigated and that other α-secretase candidates should also be taken into consideration.

Our data show that ADAM 10 is critically involved in early vertebrate embryogenesis. Its deficiency invariably causes embryonic lethality at E 9.5 associated with multiple malformations strikingly similar to that of a complex Notch deficiency as seen in *PS1*/*PS2* or *notch 1*/*notch 4* double-knockout mice (44,45,49). This effect is clearly independent of APP, since (i) mice deficient in APP or APLP2 survive up to birth and even beyond (50) and (ii) no phenotypic differences occur between embryos giving rise to APP secreting or non-secreting cell lines.

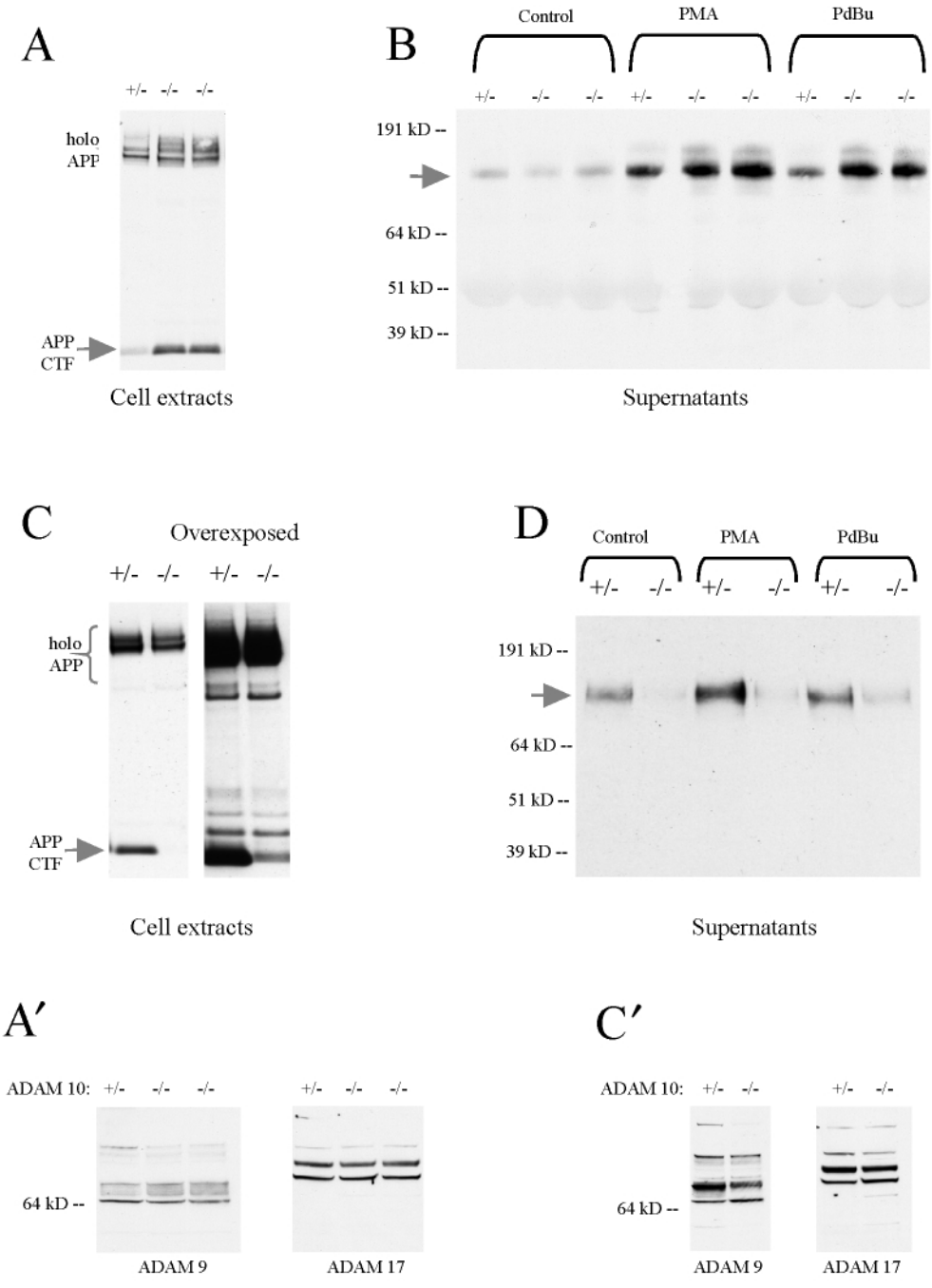

Figure 4. Constitutive and induced α secretion in 'secretor' and 'non-secretor' embryonic fibroblasts. (**A**) Western blot of cell extracts using APP C-terminus-specific antibodies performed with ADAM 10-deficient 'secretor' cell lines and demonstration of secreted APPsα in the supernatant (**B**). In these ADAM 10-deficient cell lines representing the upper extreme of the various lines generated, both the constitutive and inducible fractions were present, and were even increased above those of controls. (**C**) When the same experiment was done with 'non-secretor' ADAM 10-deficient cell lines, α-secretase-generated APP CTFs (indicated by an arrow) were virtually absent. Only after overexposure of the same blot, could a faint band be visualized, indicating a small remaining α-secretase activity in ADAM 10-deficient 'non-secretor' cell lines. (**D**) A western blot of the supernatant of the same cell lines is shown stained for APPs by the monoclonal antibody 22C11. In the first two lanes, the absence of secretion is confirmed. After treatment with the PKC activators PMA and PDBU, however, no substantial increase in secretion could be demonstrated. (**A′**) and (**C′**) Cell extracts from the same cell lines as used in (A) and (C) were assayed for ADAM 9 and ADAM 17, the main alternative α-secretase candidates. No difference in expression level could be observed between control and knockout lines.

In *Drosophila*, the ADAM 10 orthologue Kuzbanian plays a dual role in Notch signalling by shedding the Notch ligand Delta and performing the 'site2' cleavage of the receptor, initiating signal transduction after ligand binding (38, 39, 51–55). As summarized in the Introduction, several attempts to establish a similar function for ADAM 10 in the mouse have led to considerable confusion by showing that Notch cleavage (at least *in vitro*) is performed by ADAM 17 instead of

ADAM 10 (40,41), whereas the ADAM 17-deficient mouse shows no indication of a 'Notch phenotype' (43). So far, only for the *in vitro* differentiation of ADAM 17-deficient bone marrow stem cells, effects related to defective Notch signalling been reported (41).

To reconcile these contradictory data, it is conceivable that, similar to what we propose for APPα cleavage, different enzymes may contribute to notch site2 cleavage in a tissue-specific manner, and the phenotype data reported here clearly underscore a major role for ADAM 10 in this process *in vivo*, calling for a reinvestigation of ADAM 10 function in Notch signalling.

Alternatively, the 'Notch-like' phenotype of ADAM 10-deficient mice could be explained by its presumed role in ligand shedding (51,56). Delta ectodomain shedding has been suggested to induce Notch signalling in cells not immediately close to the Delta-expressing cells (51) or as a mechanism to reduce the inhibitory effects of ligands on Notch receptor ligands on the same cell (56). Additionally, ADAM 10 might exert developmentally relevant effects not involving Notch signalling, for instance via a disintegrin-like function (57,58) or cleavage of other substrates such as EGFR (59) and L1 (60). This could explain why in some tissues, such as the developing heart, ADAM 10-deficient mice are more severely affected than mice deficient for the PSs, which have (theoretically at least) completely lost the capacity for NICD generation from any Notch variant (11,44).

In summary, we provide here the first analysis of mice deficient for ADAM 10, the main candidate for APP α-secretase. At least embryonic fibroblasts were able to compensate for the loss of this activity, underscoring the involvement of several proteases in APPsα secretion and stressing the importance of regulated compensatory mechanisms in this regard. In contrast with previously published biochemical data, we provide here substantial evidence for a key function of ADAM 10 in Notch signalling in mammals. The precise molecular events remain to be clarified by further studies.

MATERIALS AND METHODS

Isolation of a genomic clone and targeting vector construction

A mouse *ADAM 10* phage clone mADAM-10/13 containing the 5′ region of the gene with one 5′ exon corresponding to cDNA position nt66 to nt206 (nucleotides are counted from the ATG starting codon) was isolated from a EMBL3–129Sv phage library (Stratagene, La Jolla, USA). For construction of a targeting vector, a 5.3 kb *Sac*I-*Eco*RV DNA restriction fragment of *ADAM 10* covering the 5′ exon [Fig. 1A(II)] was subcloned into the plasmid vector pbluescript SKII+ (Stratagene). The *neo* expression cassette from pMC1neopA (Stratagene) was inserted as a *Bam*HI DNA restriction fragment. The insertion of the *neo* cassette introduces a premature translational stop codon into the ORF of the *ADAM 10* gene.

Selection of targeted embryonic stem (ES) cells and generation of mutant mice

The targeting vector was linearized with *Xho*I and introduced into the ES cell line E14-1 by electroporation. ES cells were cultured as described previously (11). G418 resistant colonies were screened by Southern blot analysis of DNA digested with *Sac*I and hybridized with probe A (*Sac*I-*Eco*RV 0.15 kb fragment) (Fig. 1A). The mutated ES line E-ADAM-10/1 was microinjected into blastocysts of C57BL/6J mice or aggregated with morulae from CD1 mice. Chimeric males were mated to C57BL/6J females or CD1 females in the case of aggregation chimeras. Mice were genotyped for the *ADAM 10* gene mutation by Southern blot analysis of *Sac*I-digested genomic DNA, using probe A or by PCR analyses using a neomycin-specific PCR and an exon-specific PCR with primers (ADAM 10/5ex 5′-gactgttacctgtgtgcttgttt-3′ and ADAM 10/3ex 5′-agacttcagatactgagagcaatga-3′) flanking the exon used for interruption. Homozygous mutant mice were obtained by mating heterozygous mice. Double-targeted ES cells were generated by an additional electroporation using a targeting construct in which the neomycin cassette was replaced by a hygromycin cassette. Double-targeted ES cells were identified by Southern blot, PCR and western blot analyses.

RT–PCR

RT–PCR was performed using the primers ADAM 10-5′ (5′-ggaagatggtgttgccgacagtgttaat-3′) and ADAM 10-3′ (5′-gtaggcactaggaagaaccaaggcaa-3′) and the Pharmacia RT–PCR system. Total RNA of mouse embryonic fibroblasts was prepared using the Quiagen RNeasy system.

Western blot analyses

Murine embryonic fibroblasts were derived from dissociated E 9.5 embryos and maintained in DMEM/F12 supplemented with fetal calf serum and antibiotics. After careful washing to remove serum, conditioning was performed in serum-free DMEM/F12 for 4 h.

Conditioned media and cell extracts were resolved on a 4–12% BisTris gel with MES/MOPS electrophoresis buffer as indicated by the manufacturer (Novex-Invitrogen). ADAM 10 was detected using a novel polyclonal antiserum (B 42.1) generated against the 17 C-terminal amino acid residues of ADAM 10. APP holoprotein and APP fragments were detected as described previously (10). ADAMs 9 and 17 were detected by commercial polyclonal antisera (Chemicon). APP C-terminal fragments were stained by antibody B 10.4 raised against the C-terminal 20 amino acids of APP as described previously (10,18). APPs was immunoprecipitated by a polyclonal antibody (kindly donated by Dr B. Greenberg) and detected by the monoclonal antibody 22C11 (Roche, Mannheim, FRG). Blots were developed using the ECL Detection System (Amersham).

Histology

For whole-mount preparations and scanning electron microscopy (SEM), embryos were fixed in 2.5% glutaraldehyde.

Specimens for SEM were postfixed in buffered 1% OsO_4 containing 6.5% sucrose and processed according to standard procedures. Analysis was done with a Philips XL 20 scanning electron microscope.

For light microscopy, embryos were fixed by immersion in 2% paraformaldehyde or in Bouin's solution diluted 1 : 3 with 0.1 M phosphate buffer. Paraffin sections were stained with hematoxylin and eosin or incubated with antibody TER 119 (Pharmingen) detected by the avidin–biotin complex technique (reagents from Vector, Burlingame, USA).

For *in situ* hybridization, embryos fixed in 2% paraformaldehyde were processed as described above under RNase-free conditions. After prehybridization, sections were exposed to ^{35}S-labelled probes against *Notch-1*, *dll-1*, and *hes-1* and *-5*.

ACKNOWLEDGEMENTS

We thank Annegret Schneemann, Monika Grell, Marleen Regent and An Snellinx for excellent technical assistance and K. Rajewski (Köln, FRG) for providing the E-14-1 cell line. We are indebted to the Department of Anatomy of the CAU Kiel for providing generous access to the scanning electron microscope facility. We thank Dr An Zwijsen (Celgen, KU Leuven) for cDNA probes and for teaching us *in situ* hybridization. We thank Dr Danny Huylebroeck (Celgen, VIB–KU Leuven) for practical advice. This work was supported by the Deutsche Forschungsgemeinschaft, the Fonds der Chemischen Industrie, the KU Leuven, the VIB, the fifth program of the IUAP network Belgium and the FWO-Vlaanderen. W.A. is a postdoctoral researcher of the FWO-Vlaanderen.

REFERENCES

1. Haass, C. and De Strooper, B. (1999) The presenilins in Alzheimer's disease—proteolysis holds the key. *Science*, **286**, 916–919.
2. Selkoe, D.J. (1998) The cell biology of β-amyloid precursor protein and presenilin in Alzheimer's disease. *Trends Cell Biol.*, **8**, 447–453.
3. Haass, C. and Selkoe, D.J. (1993) Cellular processing of β-amyloid precursor protein and the genesis of amyloid β-peptide. *Cell*, **75**, 1039–1042.
4. Brown, M.S., Ye, J., Rawson, R.B. and Goldstein, J.L. (2000) Regulated intramembrane proteolysis: a control mechanism conserved from bacteria to humans. *Cell*, **100**, 391–398.
5. Huppert, S. and Kopan, R. (2001) Regulated intramembrane proteolysis takes another twist. *Dev. Cell*, **1**, 590–592.
6. Cupers, P., Orlans, I., Craessaerts, K., Annaert, W. and De, S.B. (2001) The amyloid precursor protein (APP)-cytoplasmic fragment generated by γ-secretase is rapidly degraded but distributes partially in a nuclear fraction of neurones in culture. *J. Neurochem.*, **78**, 1168–1178.
7. Cao, X. and Sudhof, T.C. (2001) A transcriptionally [correction of 'transcriptively'] active complex of APP with Fe65 and histone acetyltransferase Tip60. *Science*, **293**, 115–120.
8. Selkoe, D.J. (2001) Alzheimer's disease: genes, proteins, and therapy. *Physiol. Rev.*, **81**, 741–766.
9. Kimberly, W.T., Zheng, J.B., Guenette, S.Y. and Selkoe, D.J. (2001) The intracellular domain of the beta-amyloid precursor protein is stabilized by Fe65 and translocates to the nucleus in a Notch-like manner. *J. Biol. Chem.*, **276**, 40288–40292.
10. De Strooper, B., Saftig, P., Craessaerts, K., Vanderstichele, H., Guhde, G., Annaert, W., von Figura, K. and van Leuven, F. (1998) Deficiency of presenilin-1 inhibits the normal cleavage of amyloid precursor protein. *Nature*, **391**, 387–390.
11. Herreman, A., Serneels, L., Annaert, W., Collen, D., Schoonjans, L. and De Strooper, B. (2000) Total inactivation of γ-secretase activity in presenilin-deficient embryonic stem cells. *Nat. Cell Biol.*, **2**, 461–462.
12. Zhang, Z., Nadeau, P., Song, W., Donoviel, D., Yuan, M., Bernstein, A. and Yankner, B.A. (2000) Presenilins are required for γ-secretase cleavage of β-APP and transmembrane cleavage of Notch-1. *Nat. Cell Biol.*, **2**, 463–465.
13. Steiner, H., Duff, K., Capell, A., Romig, H., Grim, M.G., Lincoln, S., Hardy, J., Yu, X., Picciano, M., Fechteler, K. *et al.* (1999) A loss of function mutation of presenilin-2 interferes with amyloid β-peptide production and Notch signaling. *J. Biol. Chem.*, **274**, 28669–28673.
14. Wolfe, M.S., Xia, W., Ostaszewski, B.L., Diehl, T.S., Kimberly, W.T. and Selkoe, D.J. (1999) Two transmembrane aspartates in presenilin-1 required for presenilin endoproteolysis and γ-secretase activity. *Nature*, **398**, 513–517.
15. Esler, W.P., Kimberly, W.T., Ostaszewski, B.L., Diehl, T.S., Moore, C.L., Tsai, J.Y., Rahmati, T., Xia, W., Selkoe, D.J. and Wolfe, M.S. (2000) Transition-state analogue inhibitors of γ-secretase bind directly to presenilin-1. *Nat. Cell Biol.*, **2**, 428–434.
16. Esler, W.P. and Wolfe, M.S. (2001) A portrait of Alzheimer secretases—new features and familiar faces. *Science*, **293**, 1449–1454.
17. Li, Y.M., Xu, M., Lai, M.T., Huang, Q., Castro, J.L., DiMuzio-Mower, J., Harrison, T., Lellis, C., Nadin, A., Neduvelil, J.G. *et al.* (2000) Photoactivated γ-secretase inhibitors directed to the active site covalently label presenilin 1. *Nature*, **405**, 689–694.
18. Annaert, W.G., Levesque, L., Craessaerts, K., Dierinck, I., Snellings, G., Westaway, D., George-Hyslop, P.S., Cordell, B., Fraser, P. and De Strooper, B. (1999) Presenilin 1 controls γ-secretase processing of amyloid precursor protein in pre-Golgi compartments of hippocampal neurons. *J. Cell. Biol.*, **147**, 277–294.
19. Yu, G., Nishimura, M., Arawaka, S., Levitan, D., Zhang, L., Tandon, A., Song, Y.Q., Rogaeva, E., Chen, F., Kawarai, T. *et al.* (2000) Nicastrin modulates presenilin-mediated Notch/glp-1 signal transduction and βAPP processing. *Nature*, **407**, 48–54.
20. Sisodia, S.S., Koo, E.H., Beyreuther, K., Unterbeck, A. and Price, D.L. (1990) Evidence that β-amyloid protein in Alzheimer's disease is not derived by normal processing. *Science*, **248**, 492–495.
21. Vassar, R., Bennett, B.D., Babu-Khan, S., Kahn, S., Mendiaz, E.A., Denis, P., Teplow, D.B., Ross, S., Amarante, P., Loeloff, R. *et al.* (1999) β-Secretase cleavage of Alzheimer's amyloid precursor protein by the transmembrane aspartic protease BACE. *Science*, **286**, 735–741.
22. Hock, C., Maddalena, A., Heuser, I., Naber, D., Oertel, W., von der Kammer, H., Wienrich, M., Raschig, A., Deng, M., Growdon, J.H. *et al.* (2000) Treatment with the selective muscarinic agonist talsaclidine decreases cerebrospinal fluid levels of total amyloid beta-peptide in patients with Alzheimer's disease. *Ann. NY Acad. Sci.*, **920**, 285–291.
23. Marambaud, P., Lopez-Perez, E., Wilk, S. and Checler, F. (1997) Constitutive and protein kinase C-regulated secretory cleavage of Alzheimer's β-amyloid precursor protein: different control of early and late events by the proteasome. *J. Neurochem.*, **69**, 2500–2505.
24. Tagawa, K., Maruyama, K. and Ishiura, S. (1992) Amyloid β/A4 precursor protein (APP) processing in lysosomes. *Ann. NY Acad. Sci.*, **674**, 129–137.
25. Lopez-Perez, E., Seidah, N.G. and Checler, F. (1999) Proprotein convertase activity contributes to the processing of the Alzheimer's β-amyloid precursor protein in human cells: evidence for a role of the prohormone convertase PC7 in the constitutive α-secretase pathway. *J. Neurochem.*, **73**, 2056–2062.
26. Sambamurti, K., Sevlever, D., Koothan, T., Refolo, L.M., Pinnix, I., Gandhi, S., Onstead, L., Younkin, L., Prada, C.M., Yager, D. *et al.* (1999) Glycosylphosphatidylinositol-anchored proteins play an important role in the biogenesis of the Alzheimer's amyloid β-protein. *J. Biol. Chem.*, **274**, 26810–26814.
27. Farzan, M., Schnitzler, C.E., Vasilieva, N., Leung, D. and Choe, H. (2000) BACE2, a β-secretase homolog, cleaves at the β site and within the amyloid-β region of the amyloid-β precursor protein. *Proc. Natl Acad. Sci. USA*, **97**, 9712–9717.
28. Yan, R., Munzner, J.B., Shuck, M.E. and Bienkowski, M.J. (2001) BACE2 functions as an alternative α-secretase in cells. *J. Biol. Chem.*, **276**, 34019–34027.

29. Buxbaum, J.D., Liu, K.N., Luo, Y., Slack, J.L., Stocking, K.L., Peschon, J.J., Johnson, R.S., Castner, B.J., Cerretti, D.P. and Black, R.A. (1998) Evidence that tumor necrosis factor α converting enzyme is involved in regulated α-secretase cleavage of the Alzheimer amyloid protein precursor. *J. Biol. Chem.*, **273**, 27765–27767.
30. Lammich, S., Kojro, E., Postina, R., Gilbert, S., Pfeiffer, R., Jasionowski, M., Haass, C. and Fahrenholz, F. (1999) Constitutive and regulated α-secretase cleavage of Alzheimer's amyloid precursor protein by a disintegrin metalloprotease. *Proc. Natl Acad. Sci. USA*, **96**, 3922–3927.
31. Fahrenholz, F., Gilbert, S., Kojro, E., Lammich, S. and Postina, R. (2000) α-Secretase activity of the disintegrin metalloprotease ADAM 10. Influences of domain structure. *Ann. NY Acad. Sci.*, **920**, 215–222.
32. Koike, H., Tomioka, S., Sorimachi, H., Saido, T.C., Maruyama, K., Okuyama, A., Fujisawa-Sehara, A., Ohno, S., Suzuki, K. and Ishiura, S. (1999) Membrane-anchored metalloprotease MDC9 has an α-secretase activity responsible for processing the amyloid precursor protein. *Biochem. J.*, **343**, 371–375.
33. Goddard, D.R., Bunning, R.A. and Woodroofe, M.N. (2001) Astrocyte and endothelial cell expression of ADAM 17 (TACE) in adult human CNS. *Glia*, **34**, 267–271.
34. Karkkainen, I., Rybnikova, E., Pelto-Huikko, M. and Huovila, A.P. (2000) Metalloprotease–disintegrin (ADAM) genes are widely and differentially expressed in the adult CNS. *Mol. Cell. Neurosci.*, **15**, 547–560.
35. Kojro, E., Gimpl, G., Lammich, S., Marz, W. and Fahrenholz, F. (2001) Low cholesterol stimulates the nonamyloidogenic pathway by its effect on the α-secretase ADAM 10. *Proc. Natl Acad. Sci. USA*, **98**, 5815–5820.
36. Golde, T.E. and Eckman, C.B. (2001) Cholesterol modulation as an emerging strategy for the treatment of Alzheimer's disease. *Drug Discov. Today*, **6**, 1049–1055.
37. Hartmann, D., Tournoy, J., Saftig, P., Annaert, W. and De, S.B. (2001) Implication of APP secretases in Notch signaling. *J. Mol. Neurosci.*, **17**, 171–181.
38. Sotillos, S., Roch, F. and Campuzano, S. (1997) The metalloprotease–disintegrin Kuzbanian participates in Notch activation during growth and patterning of *Drosophila* imaginal discs. *Development*, **124**, 4769–4779.
39. Wen, C., Metzstein, M.M. and Greenwald, I. (1997) SUP-17, a *Caenorhabditis elegans* ADAM protein related to *Drosophila* KUZBANIAN, and its role in LIN-12/NOTCH signalling. *Development*, **124**, 4759–4767.
40. Mumm, J.S., Schroeter, E.H., Saxena, M.T., Griesemer, A., Tian, X., Pan, D.J., Ray, W.J. and Kopan, R. (2000) A ligand-induced extracellular cleavage regulates γ-secretase-like proteolytic activation of Notch1. *Mol. Cell*, **5**, 197–206.
41. Brou, C., Logeat, F., Gupta, N., Bessia, C., LeBail, O., Doedens, J.R., Cumano, A., Roux, P., Black, R.A. and Israel, A. (2000) A novel proteolytic cleavage involved in Notch signaling: the role of the disintegrin–metalloprotease TACE. *Mol. Cell*, **5**, 207–216.
42. Zhao, J., Chen, H., Peschon, J.J., Shi, W., Zhang, Y., Frank, S.J. and Warburton, D. (2001) Pulmonary hypoplasia in mice lacking tumor necrosis factor-α converting enzyme indicates an indispensable role for cell surface protein shedding during embryonic lung branching morphogenesis. *Dev. Biol.*, **232**, 204–218.
43. Peschon, J.J., Slack, J.L., Reddy, P., Stocking, K.L., Sunnarborg, S.W., Lee, D.C., Russell, W.E., Castner, B.J., Johnson, R.S., Fitzner, J.N. *et al.* (1998) An essential role for ectodomain shedding in mammalian development. *Science*, **282**, 1281–1284.
44. Herreman, A., Hartmann, D., Annaert, W., Saftig, P., Craessaerts, K., Serneels, L., Umans, L., Schrijvers, V., Checler, F., Vanderstichele, H. *et al.* (1999) Presenilin 2 deficiency causes a mild pulmonary phenotype and no changes in amyloid precursor protein processing but enhances the embryonic lethal phenotype of presenilin 1 deficiency. *Proc. Natl Acad. Sci. USA*, **96**, 11872–11877.
45. Krebs, L.T., Xue, Y., Norton, C.R., Shutter, J.R., Maguire, M., Sundberg, J.P., Gallahan, D., Closson, V., Kitajewski, J., Callahan, R. *et al.* (2000) Notch signaling is essential for vascular morphogenesis in mice. *Genes Dev.*, **14**, 1343–1352.
46. Montero, J.C., Yuste, L., Diaz-Rodriguez, E., Esparis-Ogando, A. and Pandiella, A. (2002) Mitogen-activated protein kinase-dependent and -independent routes control shedding of transmembrane growth factors through multiple secretases. *Biochem. J.*, **363**, 211–221.
47. Mudher, A., Chapman, S., Richardson, J., Asuni, A., Gibb, G., Pollard, C., Killick, R., Iqbal, T., Raymond, L., Varndell, I. *et al.* (2001) Dishevelled regulates the metabolism of amyloid precursor protein via protein kinase C/mitogen-activated protein kinase and c-Jun terminal kinase. *J. Neurosci.*, **21**, 4987–4995.
48. Weskamp, G., Cai, H., Brodie, T.A., Higashyama, S., Manova, K., Ludwig, T. and Blobel, C.P. (2002) Mice lacking the metalloprotease–disintegrin MDC9 (ADAM9) have no evident major abnormalities during development or adult life. *Mol. Cell. Biol.*, **22**, 1537–1544.
49. Huppert, S.S., Le, A., Schroeter, E.H., Mumm, J.S., Saxena, M.T., Milner, L.A. and Kopan, R. (2000) Embryonic lethality in mice homozygous for a processing-deficient allele of Notch1. *Nature*, **405**, 966–970.
50. Heber, S., Herms, J., Gajic, V., Hainfellner, J., Aguzzi, A., Rulicke, T., Kretzschmar, H., von, Koch, C., Sisodia, S., Tremml, P. *et al.* (2000) Mice with combined gene knock-outs reveal essential and partially redundant functions of amyloid precursor protein family members. *J. Neurosci.*, **20**, 7951–7963.
51. Qi, H., Rand, M.D., Wu, X., Sestan, N., Wang, W., Rakic, P., Xu, T. and Artavanis-Tsakonas, S. (1999) Processing of the Notch ligand Delta by the metalloprotease Kuzbanian. *Science*, **283**, 91–94.
52. Pan, D. and Rubin, G.M. (1997) Kuzbanian controls proteolytic processing of Notch and mediates lateral inhibition during *Drosophila* and vertebrate neurogenesis. *Cell*, **90**, 271–280.
53. Rooke, J., Pan, D., Xu, T. and Rubin, G.M. (1996) KUZ, a conserved metalloprotease–disintegrin protein with two roles in *Drosophila* neurogenesis. *Science*, **273**, 1227–1231.
54. Lieber, T., Kidd, S. and Young, M.W. (2002) Kuzbanian-mediated cleavage of *Drosophila* Notch. *Genes Dev.*, **16**, 209–221.
55. Kidd, S., Lieber, T. and Young, M.W. (1998) Ligand-induced cleavage and regulation of nuclear entry of Notch in *Drosophila melanogaster* embryos. *Genes Dev.*, **12**, 3728–3740.
56. Deblandre, G.A., Lai, E.C. and Kintner, C. (2001) *Xenopus* neuralized is a ubiquitin ligase that interacts with XDelta1 and regulates Notch signaling. *Dev. Cell*, **1**, 795–806.
57. Fambrough, D., Pan, D., Rubin, G.M. and Goodman, C.S. (1996) The cell surface metalloprotease/disintegrin Kuzbanian is required for axonal extension in *Drosophila*. *Proc. Natl Acad. Sci. USA*, **93**, 13233–13238.
58. Schimmelpfeng, K., Gogel, S. and Klambt, C. (2001) The function of leak and Kuzbanian during growth cone and cell migration. *Mech. Dev.*, **106**, 25–36.
59. Dong, J., Opresko, L.K., Dempsey, P.J., Lauffenburger, D.A., Coffey, R.J. and Wiley, H.S. (1999) Metalloprotease-mediated ligand release regulates autocrine signaling through the epidermal growth factor receptor. *Proc. Natl Acad. Sci. USA*, **96**, 6235–6240.
60. Mechtersheimer, S., Gutwein, P., Agmon-Levin, N., Stoeck, A., Oleszewski, M., Riedle, S., Fogel, M., Lemmon, V. and Altevogt, P. (2001) Ectodomain shedding of L1 adhesion molecule promotes cell migration by autocrine binding to integrins. *J. Cell Biol.*, **155**, 661–673.